MECSOL 2019 - Proceedings of the 7th International Symposium on Solid Mechanics,
V. Tita, A. Ferreira, M.L. Ribeiro, A. Vieira and A.T. Beck (Editors), ABCM, Sao Carlos, SP, Brazil, April 15th to 17th, 2019

Influence of hygrothermal conditioning on axial compression of filament wound cylindrical shells

Cristiano B. de Azevedo[1], Heitor F. Flores[1], José Humberto S. Almeida Jr.[2], Frederico Eggers[1], Sandro C. Amico[1]

[1]PPGE3M and PROMEC, Federal University of Rio Grande do Sul, Av. Bento Gonçalves 9500, 91501-970 Porto Alegre, RS, Brazil

[2]Mechanics and Composite Materials Department, Leibniz-Institut für Polymerforschung Dresden e.V., Hohe Straße 6, 01069 Dresden, Germany

Abstract: In certain applications, composite structures may either work underwater. Consequently, their mechanical behavior may be affected when working under an aggressive environment, particularly when the matrix has a major contribution to the mechanical behavior of the structure, i.e. with laminas oriented at off-axis angles. This study aims at assessing the hygrothermal conditioning effects on the mechanical response of filament wound (FW) composite cylinders in axial compression. Special attention will also be given to the filament winding pattern formed during manufacturing, which may also affect the structural response of the shells. Carbon/epoxy cylinders were manufactured via filament winding process with 1/1, 3/1 and 5/1 winding patterns and immersed into distilled water and artificial seawater (with salinity of ≈3,5% and pH 8.2, according ASTM D1141 standard) conditionings. Water uptake has been periodically measured. Then, axial compression tests were performed on all cylinders. Results showed that the environmental conditioning decreases the compressive strength in all winding pattern configurations, where for the winding patterns 1/1 and 5/1 conditioned in distilled water the reduction on the compressive strength was of 2.27% and 14.61%, respectively.

Keywords: environmental conditioning, filament winding pattern, composite cylinder, buckling

INTRODUCTION

Composite structures are being increasingly used in aerospace, civil, and marine high-performance engineering applications due to their excellent high specific strength and stiffness and high corrosion strength (Koussios, 2014). Structures used in the above fields are often exposed to aggressive environments during their service life and, hence, they may affect the mechanical behavior of the structure. The marine sector, in particular, is gradually replacing metallic-based structures with composites, given their lower density and higher corrosion resistance. In fact, submersible structures operate under aggressive environments, which may affect the mechanical response of the composite, which might sometimes lead to premature failure. Among the possible affected properties, an aggressive environment might influence the stability of structure under compressive load, once matrix and fiber/matrix interface play a relatively important role (Almeida Jr. et al, 2018) when off-axis oriented layers take place.

When a composite structure is operating underwater, the water absorption from the polymeric matrix influences may damage the matrix and the fiber/matrix interface. There are three possible mechanisms of moisture penetration in composite materials: diffusion involving transport of water molecules in the matrix, diffusion along the fiber/matrix interface and penetration of water through microcracks in the matrix (Tsenoglou, 2006). Indeed, the moisture absorption increases the free volume of the polymeric molecules, which may decrease the glass transition temperature of the matrix. This process has a plasticizing effect that induces a decrease in stiffness. Consequently, moisture absorption affects the behavior of a composite system when its behavior is driven by the matrix, such as off-axis laminates under axial compression (Opelt et. al.,2017).

Filament winding (FW) is the most suitable manufacturing technique for producing cylindrical composite structures. In the FW process, a roving is continuously wound onto a rotating mandrel, avoiding the need to generate overlaps to close off the fiber pre-form onto the mold. In addition, FW process has high accuracy on fiber positioning, produces parts with high fiber volume fraction, low void content and high reproducibility (Almeida Jr. et al, 2018). The high design freedom and the intrinsic orthotropy of continuous fiber-reinforced composites provide numerous possibilities to decrease weight while fulfilling load requirements of a particular structure.

Three winding trajectories are possible in FW process: circumferential (also well-known as hoop), helical and polar (Koussios, 2004). In helical filament winding, rotational movements of the mandrel and axial movements of the carriage

produce helical trajectories, where the full coverage occurs without the band having to be adjacent to the previously deposited web (as in the hoop winding). The trajectory can be a geodesic or non-geodesic curve. The geodetic trajectory between two points on a surface is defined as the curve inserted on the surface of revolution that connects two points through the smallest distance and occurs only when there is no friction (Moreno et al., 2008). These characteristics result in a repetitive pattern with diamond shape over the cylindrical surface. Each diamond constitutes a minimal periodic structure representing a unit cell, and within each unit cell one can distinguish two sections, each comprising half of the diamond and having unidirectional off-axis oriented filaments. Between these two sections, there is an undulation zone where the rovings cross themselves (Figure 1).

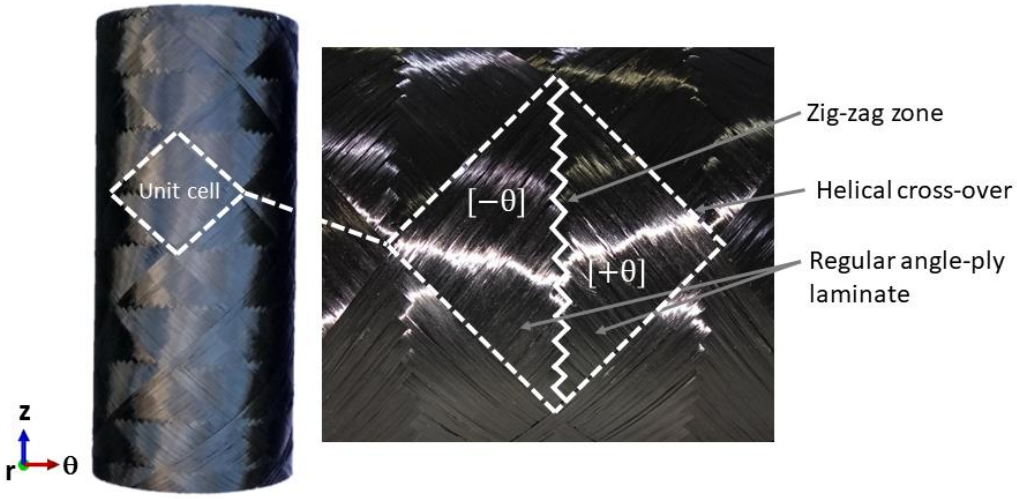

Figure 1 – Winding pattern architecture for a helical winding.

The size and arrangement of these unit cells constitute the filament winding pattern, which can be identified as a two-valued relationship, "X/Y", which means that there exist X diamonds around Y circles (Azevedo et al., 2018). Figure 2 shows three examples of cylindrical shells having the same arbitrary winding angle but with different winding patterns.

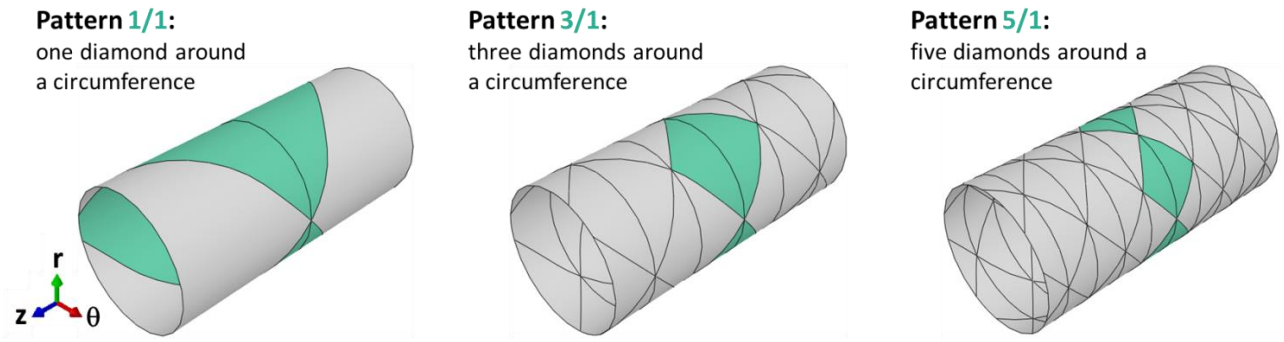

Figure 2 – Illustration of filament winding patterns.

Typically, FW structures are evaluated based on the principles of Classical Lamination Theory (CLT) and the winding pattern is usually disregarded. In such cases, a winding layer is considered as two homogenized angle-ply layers, where each $\pm\theta$ layer is divided into two $-\theta$ and $+\theta$ layers. There are a very few works accounting for winding pattern in analysis of FW structures. Among them, Morozov (2006) analyzed numerically composite cylindrical shells under internal pressure considering the winding pattern. The numerical results showed substantial differences in the stress values at the ply level calculated for the one-layered cylindrical filament-wound shells with different winding patterns. The stress distributions are not uniform along the length of the shell and its circumference and the maximum stresses acting along the fibers are higher than those calculated using conventional modelling techniques. Mian et. al. (2011) modeled numerically the winding pattern in pressure vessels subjected to internal pressure considering the winding pattern. It was found that the winding pattern have a pronounced effect on the mechanical behavior, with stress contours not uniform and maximum stress higher than those calculated using conventional FEA techniques (↑66% in the direction of fibers, for example).

In this context, this study aims at evaluate how the hygrothermal conditioning affects the mechanical response of FW composite cylinders under axial compression. Two environments are herein considered: distilled water and seawater. In addition, the effect of the filament winding pattern on the axial compressive response of the shells will be carefully investigated.

EXPERIMENTAL

Manufacturing

Cylindrical shells with winding angle of ±50, 136 mm inner diameter and 300 mm length were fabricated using towpregs from TCR Composites, based on Toray T700-12K-50C carbon fiber and UF3369 epoxy resin (Figure 3a). A 1020 steel cylindrical mandrel was used. The system was cured in an oven with air circulation at 130 ° C for 4 h. Three families were produced, each with different filament winding patterns (Figure 3b), as shows Table 1.

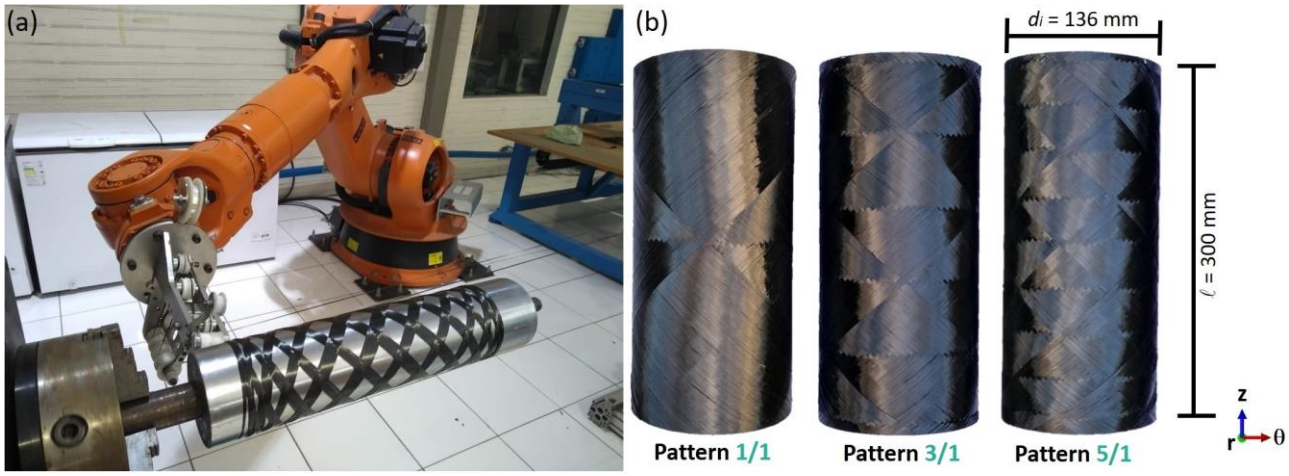

Figure 3 - Manufacturing of a cylinder (a) and cylinders produced following different winding patterns (b).

Table 1 - Geometrical characteristics of the cylinders ([±50]$_{fw}$).

Pattern number	*Mean thickness (mm)*	*Outer radius (mm)*	*r/t ratio*
1/1	0.96	68.96	71.83
3/1	0.97	68.97	71.10
5/1	0.82	68.82	83.93

Hygrothermal conditioning

The specimens were exposed to two different conditions: i) immersion in distilled water and ii) immersion in artificial sea water, both at room temperature. The artificial seawater solution, with a salinity of ≈3.5% and pH ≈8.2, was prepared following the recommendations of ASTM D1141 - 98(2013) standard.

The samples were dried before conditioning so that the initial moisture did not affect the water absorption during the conditioning. For drying, the samples were weighed, placed in an oven at 110 °C for 24 h, weighed and re-placed in an oven at 110 °C for 3 h. These steps were repeated until the samples reached mass balance. After drying and initial weighing, the samples were immersed in distilled and seawater water at room temperature for 18 days (≈400 h).

The mass of the samples was daily monitored. Three samples have been used for measuring the mass variation (Equation 1).

$$M(\%) = \frac{Final\ mass(g) - Inicial\ mass(g)}{Inicial\ mass(g)} * 100 \quad (1)$$

The moisture content for thin plates (ratio width/thickness >> 1 and length/thickness >> 1) can be predicted by deriving the first and second Fick law (Sun et. al., 2011) according to Equation (2).

$$M = M_{\infty}\left[1 - exp\left(-7.3\left(\frac{Dt}{h^2}\right)^{0.75}\right)\right] \quad (2)$$

where M_{∞} is the concentration of saturated moisture, D is the apparent diffusivity of moisture, h is the thickness and t is the time. The apparent diffusivity can be calculated from the measurements in the initial stages of diffusion, where M is proportional to the square root of time, according to Equation (3).

$$D = \pi\left(\frac{h}{4M_{\infty}}\right)^2\left(\frac{M_2 - M_1}{\sqrt{t_2} - \sqrt{t_1}}\right)^2 \quad (3)$$

Testing

Axial compression tests have been performed in an Instron Universal machine model 3382 at a crosshead speed of 2 mm/min (Figure 4). Three samples from each family were tested under three different conditions i) unconditioned (ii) conditioned with distilled water and (iii) artificial seawater.

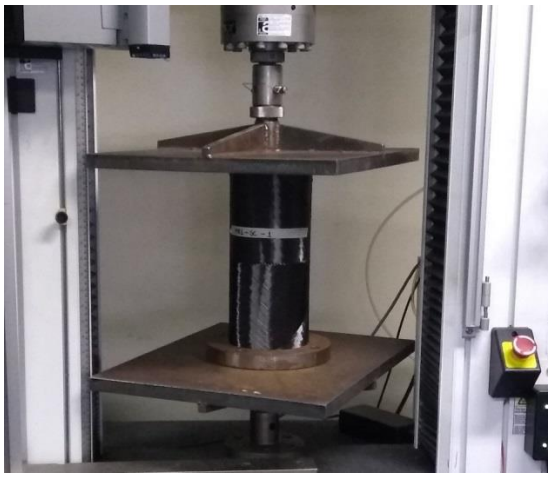

Figure 4 - Experimental set up of the axial compression test.

RESULTS AND DISCUSSION

Moisture uptake

Water moisture uptake was determined by calculating the difference between the sample weight before and after conditioning. The water absorption as a function of the immersion period is shown in Figure 5. Each point represents an average obtained from three samples.

The water uptake was well predicted by the Fickian model. After reaching the pseudo-equilibrium, absorption occurred at a lower rate, due to relaxation of the glassy epoxy network and filling of micro-avoids vitreous epoxy network, capillary action and wicking along micro-cracks in the bulk resin and along imperfect fiber–matrix interface (Karbhari et. al., 2009).

Water saturation was achieved in approximately 100 h of conditioning. The mean water uptake for conditioned samples in distilled water/artificial seawater was of 3.55 and 3.90% for the pattern 1/1, respectively; 2.47 and 2.04% for pattern 3/1, respectively; and of 3.15 and 2.88% for pattern 5/1, respectively.

A variation on the water absorption for the different conditioning has been observed, but it was not detected if the saline composition of the artificial seawater promoted an increase or decrease of the water absorption, since there was positive and negative variation.

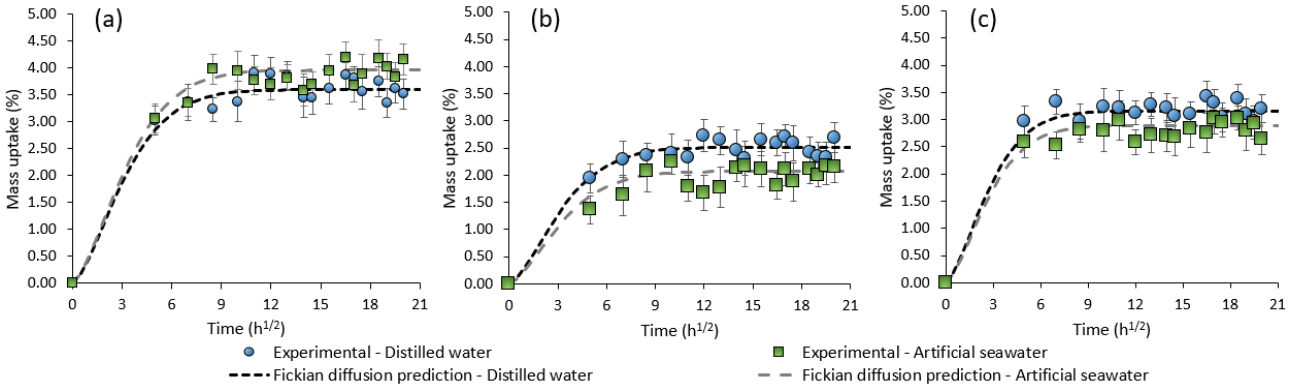

Figure 5 - Mass uptake obtained experimentally and Fickian diffusion prediction for 1/1 (a), 3/1 (b) and 5/1 (c) winding patterns.

Mechanical response and hygrothermal effects

Figure 6 shows representative load *vs.* displacement experimental curves for all cylinders studied. Firstly analyzing the environmental conditioning effects, seawater conditioning seems to have a stronger influence on the cylinders in axial compression, where this conditioning might by more detrimental to the fiber/matrix interface and, consequently, reducing

the maximum load carrying capacity. For all patterns and conditioning, the shape of the curves is very similar, which is an indicative that neither the winding pattern nor the hygrothermal conditionings change the failure mode of the cylinders.

As can be seen in Figure 6, the axial compressive behavior of the cylinders is sensitive to the mosaic winding pattern, which means that physical aspects of the sub-structure must be taken into account on the design of such structures. Amongst the three investigated winding patterns, the 3/1 one presents the highest maximum compressive load. This scenario confronts the numerical observations reported by Morozov, 2006, who carried out a stress analysis of composite cylinders under internal pressure with winding patterns comprising of 2-, 4-, and 8- triangular units. He concluded that the increase of number of triangular mosaic units and corresponding reduction in the size of each unit (4-unit and 8-unit shells) the maximum values of stresses acting along the fibers decreased.

For the winding pattern 1/1, the maximum compressive load is almost the same for unconditioned and distilled-water conditioned cylinders, whereas the cylinder conditioned with seawater has a peak load slightly lower than the other two 1/1 pattern families. For her 3/1 pattern, the same panorama is observed. On the other hand, for the pattern 5/1, the hygrothermal conditioning has a stronger influence on the peak load, since the unconditioned presents the highest peak load amongst the conditionings.

Regarding the shape of the curves after the maximum load is reached, it seems that progressive failure at the circumferential undulation zones (zig-zag regions – see Figure 1) dominates the failure of all cylinders. This failure could also be attributed to delamination-buckling triggered by local buckling at the zig-zag regions, which might be characterized by the multiple load drops after the peak load. Although a single-wall shell is herein considered, this delamination-buckling is possible considering that a ±φ angle-ply laminate is formed during the tows entanglement.

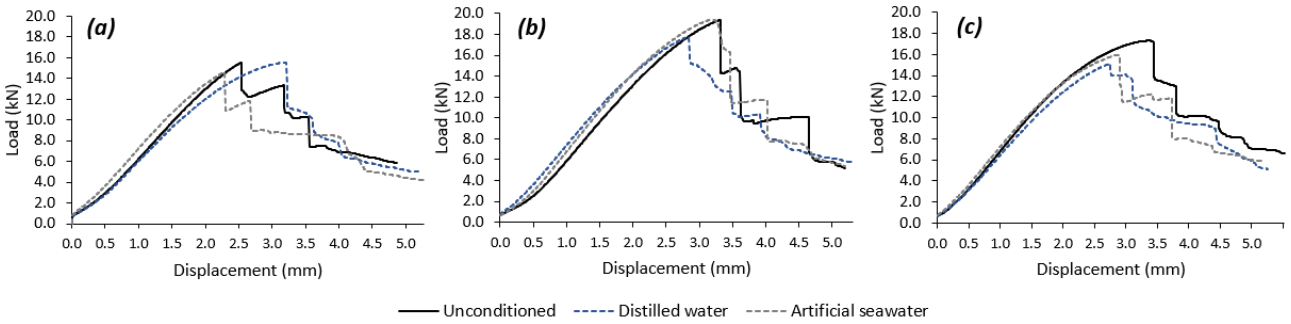

Figure 6 - Typical load *vs.* displacement experimental curves for the following winding patterns: 1/1 (a), 3/1 (b) and 5/1 (c).

Table 2 shows the compressive strength obtained for all samples. It is observed that for within each winding pattern, the compression strength reduced for post-conditioned cylinders when compared to unconditioned ones. Nevertheless, distilled water conditioning was more harmful for the winding pattern 5/1, reducing the compressive strength in 14.6%. On the other hand, seawater conditioning reduced the compressive strength in 11.7% for the 1/1 winding pattern. These reductions on the compressive strength are mainly due to matrix plasticization, micro-cracking, voids, and interfacial debonding, which are triggered by the presence of water in the micro-structure.

Table 2 – Compressive strength for all cylinders in study.

Winding pattern	*Conditioning*	*Compressive strength (MPa)*	*Variation*
1/1	Unconditioned	39.08 ± 1.56	Reference
	Distilled water	38.18 ± 1.54	↓2.27%
	Artificial seawater	34.49 ± 1.65	↓11.74%
3/1	Unconditioned	47.91 ± 2.93	Reference
	Distilled water	43.01 ± 2.02	↓10.22%
	Artificial seawater	44.29 ± 5.50	↓7.56%
5/1	Unconditioned	50.21 ± 0.57	Reference
	Distilled water	42.88 ± 0.51	↓14.61%
	Artificial seawater	45.85 ± 4.64	↓8.68%

Still analyzing results presented in Table 1, the compressive strength increases for higher winding patterns. Cylinders with larger and denser winding pattern have a greater fiber interweaving, which may increase the compressive strength of the structure. Unconditioned cylindrical shells with 3/1 and 5/1 winding patterns have compressive strength 22 and 28% higher than the 1/1 winding pattern, respectively.

Macro photographs of failed cylinders are shown in Figure 7. Localized buckled areas are identified for all cylinders, and the structure started to buckle at the zig-zag areas, which is a weaker region when compared to the regular laminate and helical transition zones (see Figure 1). The maximum load carrying capacity (see load peak in Figure 6) is reached when the localized buckling in each cylinder takes place, and after that small buckled areas are identified, which are

responsible for the subsequent load drops observed in the typical load *vs.* displacement curves. For a more detailed and conclusive failure analysis of the cylinders, micrographs at the micro level must be performed for further conclusive inferences.

Figure 7 – Final aspect of the damaged cylinders with 1/1 (a), 3/1 (b) and 5/1 (c) winding patterns.

CONCLUSION

In this study, the effect of hygrothermal conditioning on the axial compressive behavior of FW composite cylinders manufactured with different winding patterns was experimentally evaluated. Composite cylinders were submitted to hygrothermal conditioning in i) distilled water and ii) artificial seawater at room temperature. Then, all cylinders were subjected to axial compression tests.

Moisture absorption stabilized after an immersion time of 100 h. Water absorption between 2.04 and 3.90% has been achieved for the different winding patterns, and the highest uptake was obtained for cylinders wound with 1/1 winding pattern. This may be justified by the lower degree of interlacing between the tows, which allows higher water absorption between the fiber bundles.

From the axial compression tests, a reduction of up to 14% in the maximum compressive strength is reported for cylinders conditioned with distilled water, which shows that the moisture may, indeed, impair the load carrying capacity of the cylinders in axial compression. Of course, water absorption has a relatively strong influence because off-axis laminates are in charge, in which both matrix and fiber/matrix interface play a major role on the overall mechanical response of the structure.

In addition, the compressive strength is sensitive to the winding pattern, since cylindrical shells with 5/1 winding pattern exhibited a compressive strength about 28% greater than the 1/1 winding pattern. This behavior can be explained due to the greater interweaving between the layers, which is characteristic of the higher winding pattern. As a final remark, it was experimentally demonstrated that the mechanical performance of filament wound composite cylinders are dependent on the physical aspects of their substructure, namely the winding pattern.

ACKNOWLEDGMENTS

The authors would like to thank CAPES, CNPQ and FAPERGS. JHS Almeida Jr. is grateful to CAPES and Alexander von Humboldt for the financial support.

REFERENCES

Almeida Jr., J. H. S., Tonatto, M.L.P., Ribeiro, M. L., Tita, V., Amico, S.C., 2018, “Buckling and post-buckling of filament wound composite tubes under axial compression: linear, nonlinear, damage and experimental analyses”. Composites Part B, Vol. 149, pp 227-239.

Almeida Jr., J. H. S., Ribeiro, M. L., Tita, V., Amico, S.C., 2016, “Damage and failure in carbon/epoxy filament wound composite tubes under external pressure: experimental and numerical approaches”. Materials & Design, Vol. 96, pp 431-438.

Azevedo, C. B., Eggers, F., Almeida Jr., J. H. S., Amico, S. C., 2018, “Effect of the filament winding pattern modeling on the axial compression of the cylindrical shells” Proceedings of the 4th Brazilian Conference on Composite Materials, Rio de Janeiro, pp 554-561

Hernández-Moreno, H., Douchin, B., Collombet, F., Choqueuse, D., Davies, P., 2008, “Influence of winding pattern on the mechanical behavior of filament wound composite cylinders under external pressure”. Composites Science and Technology, Vol. 68, Issues 3-4, pp. 1015-1024.

Karbhari, V. M., Xian, G., 2009, "Hygrothermal effects on high VF pultruded unidirectional carbon/epoxy composites: Moisture uptake". Composites Part B, Vol. 40, pp. 41-49.

Koussios, S., 2004, “Filament Winding: a Unified Approach”. PhD Thesis, DUP Science - The Netherlands

Morozov, E. 2006, “The effect of filament-winding mosaic patterns on the strength of thin-walled composite shells”. Composite Structures, Vol. 76, pp. 123-129.

Mian, H. H., Rahman, H., 2011, “Influence of mosaic patterns on the structural integrity of filament wound composite pressure vessels”, International Journal of Structural Integrity, Vol. 2, Issue 3, pp. 345-356.

Opelt, C. V., Paiva, J. M. F., Cândido, G. M., Rezende, M. C., 2017, “A fractographic study on the effects of hygrothermal conditioning on carbon fiber/epoxy laminates submitted to axial compression”. Engineering Failure Analysis, Vol. 79, pp 342-350.

Sun, P., Zhao, Y., Luo, Y., Sun, L., 2011, “Effect of temperature and cyclic hygrothermal aging on the interlaminar shear strength of carbon fiber/bismaleimide (BMI) composite”. Materials & Design, Vol. 96, Issues 8-9, pp 4341-4347.

Tsenoglou, C. J., Pavlidou, S., Papaspyrides, C. D., 2006, "Evaluation of interfacial relaxation due to water absorption in fiber-polymer composites", Composites Science and Technology, Vol. 66, pp 2855–2864.

RESPONSIBILITY NOTICE